Scattering Function of Oligo- and Poly(methyl methacrylate)s in Dilute Solutions

Takenao Yoshizaki,† Hisao Hayashi,‡ and Hiromi Yamakawa*,†

Department of Polymer Chemistry, Kyoto University, Kyoto 606-01, Japan, and Department of Materials Chemistry, Faculty of Science and Technology, Ryukoku University, Seta, Otsu 520-21, Japan

Received December 28, 1992; Revised Manuscript Received May 1, 1993

ABSTRACT: The scattering function was measured for four samples of atactic oligo- and poly(methyl methacrylate)s (a-PMMA), each with the fraction of racemic diads $f_r = 0.79$, in the range of weight-average molecular weight M_w from 1.10×10^3 to 1.19×10^5 in acetonitrile at 44.0 °C (Θ) for the magnitude k of the scattering vector smaller than 1 Å^{-1} by the use of a point-focusing small-angle X-ray scattering (SAXS) camera. Supplementary measurements were also carried out on the sample with $M_w = 1.19 \times 10^5$ in benzene (good solvent) at 25.0 °C in order to examine the solvent effect. The Kratky plot of the present data for the high-molecular-weight samples in the Θ solvent exhibits the first maximum and minimum as observed by Kirste and Wunderlich for syndiotactic PMMA (with $f_r \simeq 0.9$). However, in the range of larger k, the former exhibits only a slight inflection, while the latter exhibits strong oscillation. A comparison is made of the present SAXS data with literature data for small-angle neutron scattering for a-PMMA in the bulk. It is found that the Kratky plots of these two kinds of data are in good agreement with each other in the range of small k but the latter plot deviates downward from the former for larger k because of the difference in the distribution of scatterers. A comparison of the present SAXS data with the helical wormlike (HW) chain theory shows that it may reproduce the data quantitatively in the range of rather small k but only qualitatively in the range of large k. A comparison is also made of the present data for a-PMMA with the previous data for atactic polystyrene in cyclohexane at 34.5 °C (Θ). It is then found that the HW theory may well explain the difference in the Kratky plot between the two polymer chains in the range of small k arising from that in the local conformation.

Introduction

Long ago, Kirste and Wunderlich[1,2] reported the experimental result that the Kratky plot of the scattering function P_s determined from small-angle X-ray scattering (SAXS) exhibits remarkable oscillation in the range of the magnitude k of the scattering vector larger than ca. 0.1 Å^{-1} for syndiotactic poly(methyl methacrylate) (s-PMMA) (with the fraction of racemic diads $f_r \simeq 0.9$) in dilute solution. Since then there have been several attempts to give a theoretical explanation of this oscillation, considering it to reflect the local chain conformation of s-PMMA.

Kirste himself[3,4] considered that the local conformation of the s-PMMA chain in dilute solution is just like a "thread with persistence of curvature". Subsequently, Flory and his co-workers[5–8] made an extensive study of the conformational properties of PMMA chains on the basis of the rotational isomeric state (RIS) model.[9] It was then shown that the characteristic ratios of the atactic (a) PMMA chain with a rather large value of f_r and also of the s-PMMA chain as a function of chain length have a maximum[6] and that the Kratky plots for them exhibit oscillation,[8] as observed by Kirste and Wunderlich.[1,2] We ourselves also made a similar study on the basis of the helical wormlike (HW) chain model[10,11] and showed that although the maximum in the characteristic ratio as predicted by the RIS model may be reproduced,[12] the second maximum and minimum in the Kratky plot cannot be predicted.[13]

Recently, we have reinvestigated P_s of the HW chain[14] in order to clarify the reason it cannot reproduce the experimental results above, examining in some detail the effect of the discrete distribution of scattering centers on the chain contour. However, we have predicted only the existence of a slight inflection in the Kratky plot in the range of k where Kirste and Wunderlich found the second maximum. This disagreement between the HW theory and experiment for P_s is difficult to understand, since in a series of our recent experimental work on dilute solution properties of oligomers and polymers[15] it has been shown that the HW chain model may well mimic the local chain conformation of real polymers on the bond-length or somewhat longer scales. Recall that the HW theory may reproduce completely the dependence on the degree of polymerization x of the ratio of the mean-square radius of gyration $\langle S^2 \rangle$ to x for a-PMMA with $f_r = 0.79$ (see Figure 6 of ref 16).

On the experimental side, the SAXS measurements by Kirste and Wunderlich were performed with a Kratky camera, and necessarily the desmearing procedure was employed in the determination of P_s from raw (smeared) scattering data. As mentioned in a previous paper,[17] this procedure may be considered inadequate for a determination of P_s in the range of large k under consideration. Moreover, the second maximum of that kind has not been observed in the small-angle neutron scattering (SANS) experiment recently made by Dettenmaier et al.[18] Thus it is very desirable to determine P_s experimentally without desmearing. This may resolve our difficulty.

In the previous study,[17] we have carried out SAXS measurements on atactic oligo- and polystyrene (a-PS) samples with a point-focusing camera instead of a Kratky camera to determine P_s rather accurately in the range of $k \lesssim 0.5$ Å^{-1} without desmearing. Thus, in the present work, with the same point-focusing camera, we determine P_s for well-characterized a-PMMA samples (with $f_r = 0.79$) in acetonitrile at 44.0 °C (Θ) and compare the results with the HW theory. Recall that for the same system, $\langle S^2 \rangle$ and the intrinsic viscosity $[\eta]$ have already been determined.[16,19] Now this camera may cover the range of $k <$ 0.5 Å^{-1} if the Cu Kα line (of wavelength $\lambda_0 = 1.54$ Å) is used

* To whom all correspondence should be addressed.
† Kyoto University.
‡ Ryukoku University.

0024-9297/93/2226-4037$04.00/0

Table I. Values of M_w, x_w, M_w/M_n, and $\langle S^2\rangle^{1/2}$ for Atactic Oligo- and Poly(methyl methacrylate)s

sample	M_w	x_w	M_w/M_n	$\langle S^2\rangle^{1/2}$, Å
OM11[a]	1.10×10^3	11.0	1.04	7.4[9][c]
OM30	2.95×10^3	29.5	1.06	14.1
MM1[b]	1.09×10^4	109	1.06	27.6
MM12	1.19×10^5	1190	1.09	87.5

[a] M_w's of OM11 and OM30 had been determined from LS in acetone at 25.0 °C.[16] [b] M_w's of MM1 and MM12 had been determined from LS in acetonitrile at 44.0 °C.[16] [c] All values of $\langle S^2\rangle^{1/2}$ had been determined from SAXS in acetonitrile at 44.0 °C.[16]

as an X-ray source, as in the previous study. For the present purpose, however, the data in the range of $k \lesssim 1$ Å^{-1} are needed, since the second maximum and minimum, if they appear, may be observed at $k \gtrsim 0.5$ Å^{-1}. In the present work, therefore, we use the Mo Kα line (of $\lambda_0 = 0.711$ Å) instead of Cu Kα to cover such a range of k. SAXS measurements are also carried out for a benzene solution of a-PMMA in order to make a direct comparison with the data by Kirste and Wunderlich.

Experimental Section

Materials. The four a-PMMA samples used in this work are the same as those used in the previous studies[16,19] of $\langle S^2\rangle$ and $[\eta]$, i.e., the fractions separated by gel permeation chromatography and/or fractional precipitation from the original whole samples prepared by group-transfer polymerization. The values of f_r for these samples are 0.79, as already mentioned. The values of the weight-average molecular weight M_w determined from light scattering (LS),[16] the weight-average degree of polymerization x_w, the ratio of M_w to the number-average molecular weight M_n, and the root-mean-square radius of gyration $\langle S^2\rangle^{1/2}$ determined from SAXS in acetonitrile at 44.0 °C (Θ)[16] are summarized in Table I.

The solvents acetonitrile and benzene used for SAXS measurements were purified according to standard procedures.

Small-Angle X-ray Scattering. As in the previous SAXS study,[17] all measurements were carried out by the use of a point-focusing camera of overall length 6 m in the High-Intensity X-ray Laboratory of Kyoto University. A detailed specification of this camera has already been given elsewhere,[20] and a brief description has been given in the previous paper.[17] Thus we here note only a few points pertinent to the present work.

In this work, the Mo Kα line of $\lambda_0 = 0.711$ Å was used as the incident beam by eliminating other lines with Zr foil of 50-μm thickness. The distance from a sample cell to a detector (two-dimensional position-sensitive proportional counter) was ca. 640 mm, as before,[17] so that intensity measurements could be carried out in the range of k up to ca. 1 Å^{-1}. The temperature of the sample cell was kept constant at 44.0 ± 0.2 °C for the acetonitrile solutions and at 25.0 ± 0.1 °C for the benzene solution. The excess scattering intensity in the range of $k \gtrsim 0.5$ Å^{-1} was very small. Therefore, in order to diminish statistical errors in this range, the intensities scattered from each solution and the solvent were accumulated for ca. 12 and 6 h, respectively. The measurements on the solvent were made before and after every measurement on the solution.

As in the previous study,[17] the two-dimensional data thus obtained for a solution of solute mass concentration c (in g/cm^3) were first corrected for the detector sensitivity and then averaged over polar angles in the detector plane to obtain the scattering intensity $I_{obs}(k, c)$ as a function of k, which is explicitly defined by

$$k = (4\pi/\lambda_0)\sin(\theta/2) \tag{1}$$

with θ the scattering angle. From the observed intensity I_{obs}, we evaluate the reduced intensity $I_R(k, c)$ defined by

$$I_R(k, c) = I_{obs}(k, c)/AI_0 \tag{2}$$

where A is the transmittance of a given sample solution and I_0 is the intensity of the incident beam monitored by the intensity scattered from a polyethylene film placed in front of the detector.

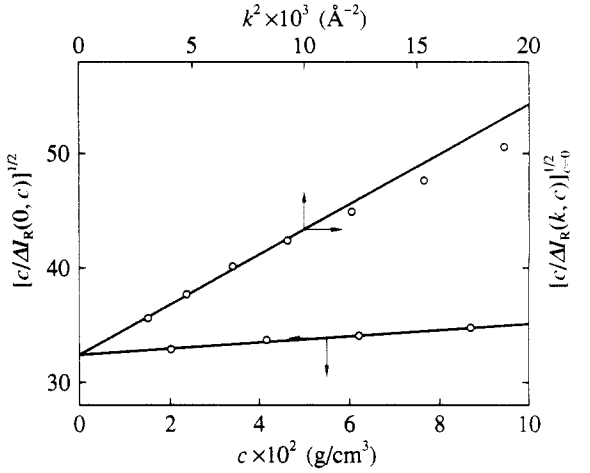

Figure 1. Plots of $[c/\Delta I_R(0, c)]^{1/2}$ and $[c/\Delta I_R(k, c)]^{1/2}_{c=0}$ against c and k^2, respectively, for sample OM30 in acetonitrile at 44.0 °C.

The excess reduced scattering intensity $\Delta I_R(k, c)$ is then obtained as the reduced scattering intensity from the solution $I_{R,soln}(k, c)$ minus that from the solvent $I_{R,solv}(k)$ [$=I_{R,soln}(k, 0)$] as follows:

$$\Delta I_R(k, c) = I_{R,soln}(k, c) - I_{R,solv}(k) \tag{3}$$

Results

We first evaluate the (normalized) scattering function P_s from the values of the reduced scattering intensity $\Delta I_R(k, c)$, which were directly obtained from SAXS measurements, in the same manner as used previously.[17]

The quantity $\Delta I_R(k, c)$ may be written in terms of P_s as

$$\frac{Kc}{\Delta I_R(k, c)} = \frac{1}{M_w P_s(k)} + 2A_2Q(k)c + \mathcal{O}(c^2) \tag{4}$$

where K is the optical constant, A_2 is the second virial coefficient, and Q represents the intermolecular interference.[21] Note that P_s and Q become unity at $k = 0$. From eq 4, we obtain

$$\frac{\Delta I_R(k, c)}{KM_w c} = P_s(k) - 2A_2M_w[P_s(k)]^2Q(k)c + \mathcal{O}(c^2) \tag{5}$$

We may then evaluate P_s by extrapolating the ratio $\Delta I_R(k, c)/KM_w c$ to $c = 0$ if the value of K is known. In the limits of $k \to 0$ and $c \to 0$, we have from eq 4

$$K = [\Delta I_R(0, c)/c]_{c=0}/M_w \tag{6}$$

Thus K may be evaluated experimentally if the value of $[\Delta I_R(0, c)/c]_{c=0}$ is determined for a sample whose M_w is known.

In the present case, we evaluated $[\Delta I_R(0, c)/c]_{c=0}$ for the sample OM30 in acetonitrile at 44.0 °C by the use of the Berry square-root plot.[22] For each solution of this sample, the plot of $(c/\Delta I_R)^{1/2}$ against k^2 followed a straight line in the range of small k, so that the intercept $[c/\Delta I_R(0, c)]^{1/2}$ at a given c could be unambiguously determined. Similarly, in the range of small k, the plot of $(c/\Delta I_R)^{1/2}$ against c was fitted by a straight line and could be extrapolated to infinite dilution to evaluate $[c/\Delta I_R(k, c)]^{1/2}_{c=0}$ at a given (small) k. The values of $[c/\Delta I_R(0, c)]^{1/2}$ and $[c/\Delta I_R(k, c)]^{1/2}_{c=0}$ thus determined for the sample OM30 are plotted against c and k^2, respectively, in Figure 1. The two kinds of plots can be extrapolated to obtain the common intercept $[c/\Delta I_R(0,c)]^{1/2}_{c=0} = 32.4$ (g/cm^3)$^{1/2}$. With the value of M_w for the sample OM30 given in Table I, K is thus evaluated to be 3.23×10^{17} cm^3/g.

Before presenting results for the scattering function, we here make one remark. From the intercept and initial

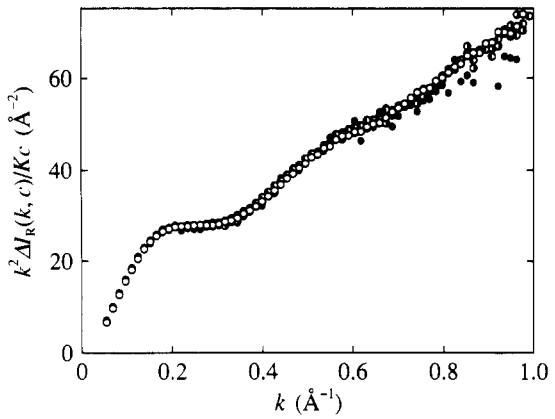

Figure 2. Plots of $k^2\Delta I_R(k, c)/Kc$ against k for sample OM30 in acetonitrile at 44.0 °C: (○) c = 0.0870 g/cm^3; (◑) c = 0.0621 g/cm^3; (◐) c = 0.0416 g/cm^3; (●) c = 0.0202 g/cm^3.

slope of the plot of $[c/\Delta I_R(k, c)]_{c=0}^{1/2}$ against k^2 in Figure 1, we may determine the apparent mean-square radius of gyration $\langle S^2\rangle_s$ defined in the equation

$$P_s(k) = 1 - (1/3)\langle S^2\rangle_s k^2 + \mathcal{O}(k^4) \quad (7)$$

The result for $\langle S^2\rangle_s$ thus obtained is 203 Å^2. This value is in good agreement with the corresponding value 207 Å^2 determined previously,[16] indicating the consistency between the present and previous determinations of the scattering intensity in the range of small k. (Note that $\langle S^2\rangle_s$ should in general be distinguished from the mean-square radius of gyration $\langle S^2\rangle$ of the chain contour except for a long enough chain.[16])

Now, Figure 2 shows plots of $k^2\Delta I_R(k, c)/Kc$ against k for the sample OM30 in acetonitrile at various c at 44.0 °C. The ordinate quantity corresponds to the (absolute-scale) Kratky function $F_s(k)$ defined by

$$F_s(k) = M_w k^2 P_s(k) \quad (8)$$

(at finite concentrations), the above plot being just the Kratky plot. In the figure, the unfilled, right-half-filled, left-half-filled, and filled circles represent the values at c = 0.0870, 0.0621, 0.0416, and 0.0202 g/cm^3, respectively. It is seen that the plot is almost independent of c in the range of k displayed, so that we adopt the values of $\Delta I_R(k, c)/KM_w c$ at the highest concentration as those of the scattering function P_s for the single polymer chain at infinite dilution. Note that in the range of small k, the concentration dependence is appreciable in the plot displayed in Figure 1 but cannot be recognized in the Kratky plot. We must also note that for a-PS in cyclohexane at 34.5 °C, the Kratky plot depends appreciably on c in the range of $k \gtrsim 0.1$ Å^{-1}, in contrast to the present case of a-PMMA.

Figure 3 shows plots of $F_s(k)$ against k for all the a-PMMA samples in acetonitrile at 44.0 °C, where the data points for the samples OM30, MM1, and MM12 have been shifted upward by 20, 40, and 60 Å^{-2}, respectively, for convenience. The plot exhibits clearly the first maximum and minimum for the sample MM1 and a slight inflection (or bump) at k = 0.5–0.6 Å^{-1} for the samples OM30 through MM12.

Discussion

Kratky Function. As shown in Figure 3, the data for the function F_s in the range of $k \lesssim 0.05$ Å^{-1} could not be obtained under the present condition of setting the sample-to-detector distance of the SAXS camera mentioned in the Experimental Section. (Note that the smallest attainable scattering angle θ in the present measurements is about half that in the previous measurements on a-PS. This difference is due to the difference in the tuning of the collimation.) Thus we join the present data to the previous data[16] obtained for F_s in the range of small k by the use of a Kratky camera.

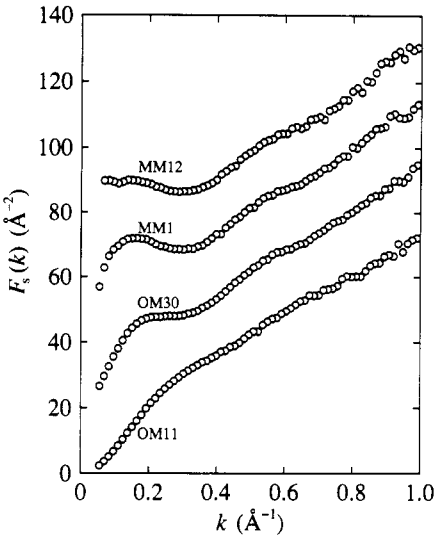

Figure 3. Plots of $F_s(k)$ against k for all the samples in acetonitrile at 44.0 °C, the data points for samples OM30, MM1, and MM12 being shifted upward by 20, 40, and 60 Å^{-2}, respectively.

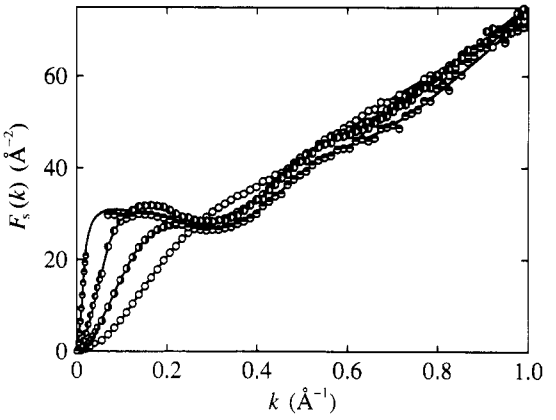

Figure 4. Plots of $F_s(k)$ against k for all the samples in acetonitrile at 44.0 °C: (○) OM11; (◑) OM30; (◐) MM1; (●) MM12. The large and small circles represent the present and previous[16] data, respectively. The solid curve connects smoothly the data points for each sample.

Figure 4 shows plots of the data for F_s thus obtained against k for the four a-PMMA samples in acetonitrile at 44.0 °C. The unfilled, right-half-filled, left-half-filled, and top-half-filled circles represent the values for the samples OM11, OM30, MM1, and MM12, respectively, the large and small circles representing the present and previous data, respectively. It is seen that the present data may be smoothly joined to the previous data for the samples OM11 through MM1, although the two kinds of data points do not overlap with each other for the sample MM12. This confirms the appropriateness and accuracy of the present determination of F_s described in the Results. Thus the solid curve connects smoothly the data points for each sample.

It is seen that F_s first increases from zero with increasing k and then exhibits the maximum (and minimum) for $M_w \gtrsim 3 \times 10^3$, that F_s is larger for larger M_w at fixed $k \lesssim 0.1$ Å^{-1} (before reaching the maximum), and that the value of k at which F_s has its maximum decreases with increasing M_w. The existence of this maximum may be considered

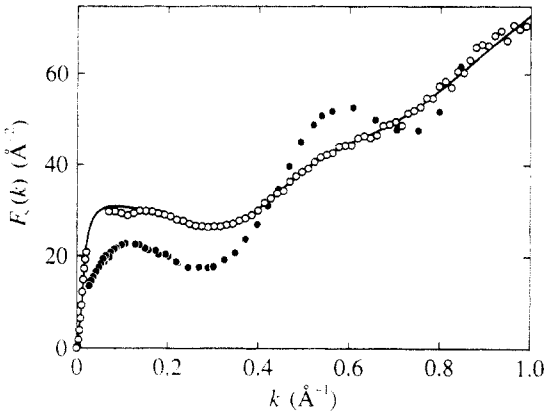

Figure 5. Comparison between the SAXS data obtained with a point-focusing camera in this work and those with a Kratky camera with desmearing: (○) present data for sample MM12 in acetonitrile at 44.0 °C; (●) desmeared data by Kirste and Wunderlich[1,2,23] for an s-PMMA sample with $M_w = 2.7 \times 10^5$ in benzene (see the text). The solid curve connects smoothly the present data points.

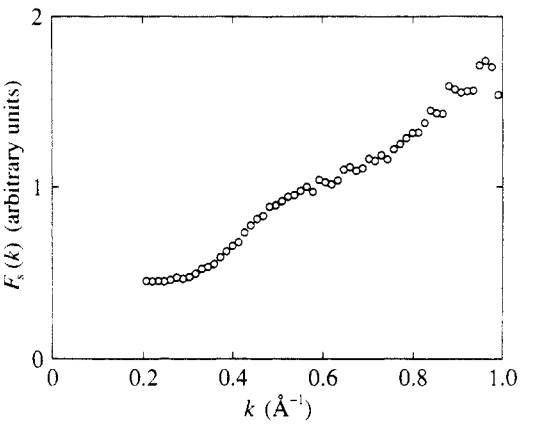

Figure 6. Plot of $F_s(k)$ against k for sample MM12 in benzene at 25.0 °C.

to reflect the local conformation of the a-PMMA chain, and it is discussed in detail later. On the other hand, the behavior of F_s is rather insensitive to a change of M_w in the range of $k \gtrsim 0.4$ Å^{-1}, although the inflection (or bump) exists at $k = 0.5$–0.6 Å^{-1} for $M_w \gtrsim 3 \times 10^3$, as mentioned in the Results. This is in contrast to the case of a-PS for which F_s depends appreciably on M_w for $M_w \lesssim 10^4$ in the range of $k \gtrsim 0.2$ Å^{-1}. This implies that the environment around the a-PMMA chain is independent of M_w.

Comparison with Desmeared SAXS Data. Now we make a comparison of the present SAXS data for F_s with the desmeared data obtained by Kirste and Wunderlich.[1,2] Figure 5 shows plots of F_s against k, where the unfilled and filled circles represent our data for the sample MM12 in acetonitrile at 44.0 °C and theirs for an s-PMMA sample with $M_w = 2.7 \times 10^5$ in benzene, respectively.

The latter plot, which has been reproduced from Figure 8 of the previous paper,[13] requires some remarks. Since the data for the relative-scale Kratky function had only been given in their original papers,[1,2] we constructed previously[13] that plot by connecting them with those for the absolute-scale F_s given in the range of $k \lesssim 0.3$ Å^{-1} in Figure 4 of Kirste et al.'s paper,[23] as done by Yoon and Flory.[8] Subsequently, however, Kirste and Oberthür[24] used the data of the same source as above to construct a plot of F_s, the absolute intensity for which is ca. 25% smaller than that for the above plot. We do not know which of the two plots[23,24] is correct. Then the adoption of the former plot[23] is only a matter of convenience. Thus we here do not discuss the absolute intensities themselves but only the shapes of the plots.

Although both of the plots exhibit the first maximum and minimum, the forms of the maxima, especially those of the shoulders on their left side, are very different from each other. However, the excluded-volume effect exists in the benzene solution, and therefore we cannot directly compare the shapes of the two plots in the range of small k.

Now it is seen that the second maximum and minimum as observed by Kirste and Wunderlich do not exist in the present data, as already often mentioned; only a slight inflection can be observed in the latter at $k \simeq 0.55$ Å^{-1} where the second maximum is observed in the former. Then the difference between the two samples in M_w has no significant effect on that in the behavior of F_s in the range of large k, as seen from Figure 4. Further, their results for a-PMMA in benzene (as shown in Figure 9 of ref 2) also show the strong oscillation in the range of large k, although there are no data in the range of k where the second minimum must be observed. (We do not reproduce these results since they have not been given on the absolute scale.) Thus the disagreement in the range of large k probably is not due to the difference in f_r either but to some other source, for instance, the difference in solvent or data processing. In order to examine the effect of solvent, we have therefore carried out supplementary measurements on a benzene solution of the sample MM12 at $c = 0.0263$ g/cm^3 at 25.0 °C in the range of $k \geq 0.2$ Å^{-1}, although the absolute intensity has not been determined. Its (relative-scale) F_s is plotted against k in Figure 6. As in the case of the acetonitrile solution, only a slight inflection (or bump) instead of a (second) maximum is observed. Thus another possible source of the above disagreement seems to be the desmearing procedure adopted by them, which we believe is inadequate for large k. However, we cannot completely reject the effect of the difference in f_r at the present time, and therefore we plan to carry out SAXS measurements on s-PMMA by the use of a point-focusing camera in the near future.

Concerning the above second maximum and minimum, it is pertinent to refer here to the RIS theoretical results. The scattering function for s-PMMA (with $f_r = 1$) was first calculated by Yoon and Flory[8] on the basis of the two-state RIS model,[5] choosing the α carbon atoms as the scattering centers. Their result for $F_x(k)$ [$=F_s(k)/M_0$ with M_0 the molecular weight per repeat unit] predicts the second maximum and minimum as observed by Kirste and Wunderlich, although the values of k at which the first and second maxima appear are appreciably smaller than the observed values. In the previous study,[14] we have examined the dependence on f_r of F_x in the range of large k on the basis of the two-state RIS model as above and also of the three-state model recently proposed by Sundararajan.[25] For both models, the amplitude of the oscillation in the range of large k becomes small as f_r is decreased (see Figures 3 and 4 of ref 14). For a given f_r, the amplitude for the three-state model is smaller than that for the two-state one. For the two-state model, the second maximum and minimum almost disappear for $f_r = 0.8$, although there still remains a remarkable inflection. As for the three-state model, the inflection becomes very weak for $f_r = 0.8$, and the form of the Kratky plot then becomes rather close to the present experimental results. As pointed out previously,[14] however, the above RIS models with $f_r = 0.8$ cannot explain the observed maximum[16] of $\langle S^2 \rangle / x$ as a function of x. For $f_r = 0.9$ corresponding to the sample used by Kirste and Wunderlich, both of the

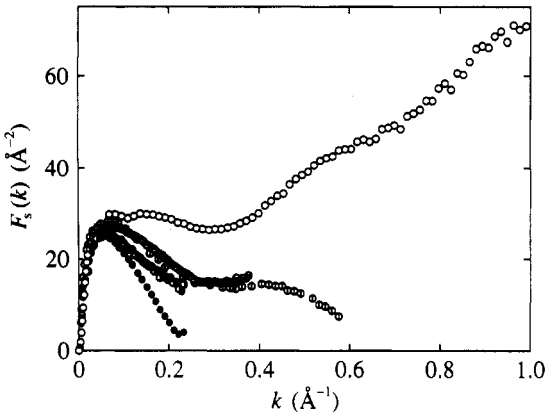

Figure 7. Comparison between SAXS and SANS data for a-PMMA with $M_w = 1.0 \times 10^5$–2.5×10^5: (○) present SAXS data for sample MM12 in acetonitrile at 44.0 °C; (●) SANS data by Kirste et al.;[23] (◑) by O'Reilly et al.;[28] (⊘) by Dettenmaier et al.;[18] (⊖) by Ito et al.[29]

two models still predict the second maximum and minimum, but the amplitude of the oscillation is smaller than that in their experimental data. Very recently, Vacatello et al.[26] calculated F_z on the basis of the six-state RIS model.[27] As in the case of the three-state model, the amplitude of its oscillation seems to become small compared to that for the two-state model. However, we note that this model also fails to predict the maximum of $\langle S^2 \rangle / x$ observed for $f_r \simeq 0.8$.[16] These RIS results are again referred to later in a comparison of the present data with the HW theory.

Comparison with SANS Data. Next we proceed to make a comparison of the present SAXS data for F_s with SANS data. It is shown in Figure 7, where the unfilled circles represent the present SAXS data for the sample MM12 in acetonitrile at 44.0 °C and the other circles the SANS data for a-PMMA samples in the bulk, all with $f_r \simeq 0.8$ and with $M_w = 10^5$–2.5×10^5. The filled circles represent the data by Kirste et al.,[23] the right-half-filled circles the data by O'Reilly et al.,[28] the circles with a vertical line segment the data by Dettenmaier et al.,[18] and the circles with a horizontal line segment the data by Ito et al.[29] As for the data by O'Reilly et al., we have adopted those corrected by Vacatello et al.[26]

Except for the data by Kirste et al. in the range of $k \gtrsim 0.1$ Å^{-1}, all the SANS data agree well with each other within experimental errors. The present SAXS data are in good agreement with the SANS data in the range of $k \lesssim 0.05$ Å^{-1}, i.e., on the left side of the first maximum (or shoulder). This indicates that the conformation of the a-PMMA chain in the bulk is quite similar to that of the isolated chain in the Θ solvent, acetonitrile at 44.0 °C, in conformity with the common notion. The disagreement between the SAXS and SANS data in the range of large k may be considered to arise from the difference between the two kinds of experiments in the distribution of scatterers. For SAXS, the scatterers (electrons) may be considered to distribute in rather small regions around the α carbon atoms and the ester groups. On the other hand, for SANS, the scatterers are the hydrogen nuclei. Thus the effective thickness of the chain is smaller for SAXS than for SANS, so that F_s in the range of large k becomes larger for the former than for the latter. (A quantitative discussion is given in the next subsection.)

Comparison with the HW Theory. Now we are in a position to make a comparison of the present experimental data for F_s with the corresponding theory for the HW chain. The latter has been developed in the previous paper,[14] where the effect of chain thickness [i.e., thickness of the distribution of electrons (or hydrogen nuclei) around the HW chain contour] has been taken into account by assuming the two simple models for this distribution, i.e., the cylinder model and the touched-spheroid model. As in the case of the previous analysis of the SAXS data for a-PS,[17] we consider here only the former model, for simplicity.

The scattering function $P_s(k; L)$ for the HW chain of total contour length L is given by eq 25 with eqs 36–41 of ref 14 and may be written in the form

$$P_s(k; L) = 2L^{-2} \int_0^L (L - t) I(\mathbf{k}; t) \{ [F_0(kd)]^2 + g_2^{00}(t) [F_1(kd)]^2 \} \, dt \quad (9)$$

where $I(\mathbf{k}; t)$ is the characteristic funtion, i.e., the Fourier transform of the distribution function $G(\mathbf{R}; t)$ of the end-to-end vector distance $\mathbf{R}$ for the HW chain of contour length t, F_n ($n = 0, 1$) are the functions given by eqs 40 and 41 of ref 14 representing the effects of the distribution of electrons (or hydrogen nuclei) within a (flexible) cylinder of diameter d, and g_2^{00} is the angular correlation function[30] given by eq 38 of ref 14. The functions I and g_2^{00} are dependent also on the three basic model parameters of the HW chain: the constant curvature κ_0 and torsion τ_0 of its characteristic helix taken at the minimum zero of its elastic energy and the static stiffness parameter λ^{-1}. We note that the function I may be evaluated numerically by the use of the weighting function and ϵ methods,[31] so that the integration over t in eq 9 must be carried out numerically. In order to compare the theoretical values of P_s as a function of k for given values of L and d with the experimental values, L may be converted to M_w by the use of the relation

$$L = M_w / M_L \quad (10)$$

with M_L the shift factor as defined as the molecular weight per unit contour length. The Kratky function F_s may then be calculated theoretically from eq 8 with eq 9. All numerical work has been done by the use of a Fujitsu M-1800/30 digital computer in Kyoto University.

In the previous case of a-PS,[17] the experimental data for F_s in the range of $k \lesssim 0.25$ Å^{-1} has been well reproduced by the theory using the values of the HW model parameters determined from an analysis[32] of $\langle S^2 \rangle$ along with that of d properly assigned. In the present case for a-PMMA, however, the agreement between theory and experiment is not complete even in such a range of small k that the effet of d may be neglected, if we use the parameter values $\lambda^{-1}\kappa_0 = 4.0$, $\lambda^{-1}\tau_0 = 1.1$, $\lambda^{-1} = 57.9$ Å, and $M_L = 36.3$ Å^{-1} determined from $\langle S^2 \rangle$.[16] Thus we redetermine here the values of λ^{-1} and M_L so that the theory may well agree with the experimental results for all four a-PMMA samples in such a range of small k, keeping the above values of $\lambda^{-1}\kappa_0$ and $\lambda^{-1}\tau_0$ unchanged. Note that the theoretical curve of $\langle S^2 \rangle / x$ as a function of x exhibits a maximum as far as these two values are unchanged. The former two values thus redetermined are $\lambda^{-1} = 47.0$ Å and $M_L = 38.0$ Å^{-1}. These values are rather close to the results $\lambda^{-1} = 45.0$ Å and $M_L = 38.6$ Å^{-1} determined from $[\eta]$[19] and may be considered to be within the limits of allowance.

Figure 8 shows plots of F_s against k for the a-PMMA sample MM1 in acetonitrile at 44.0 °C. The unfilled circles represent the experimental values and the solid curves the corresponding HW theoretical values (for $L =$ 267 Å) calculated from eq 8 with eq 9 with the values of the model parameters mentioned above and those of λd indicated. It is seen that the theory may well reproduce the experimental data in the range of $k \lesssim 0.1$ Å^{-1} but fails

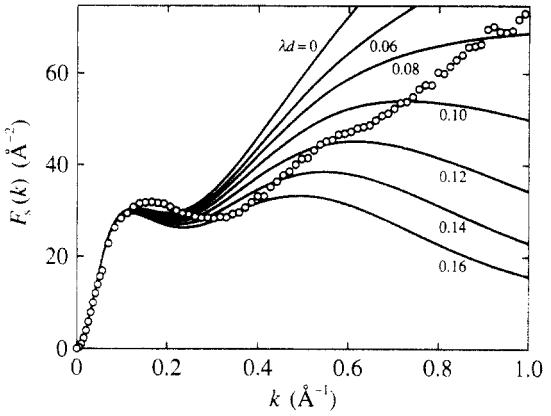

Figure 8. Comparison of the observed values of F_s for sample MM1 with the HW theoretical values: (O) data in acetonitrile at 44.0 °C; (solid curves) HW theoretical values.

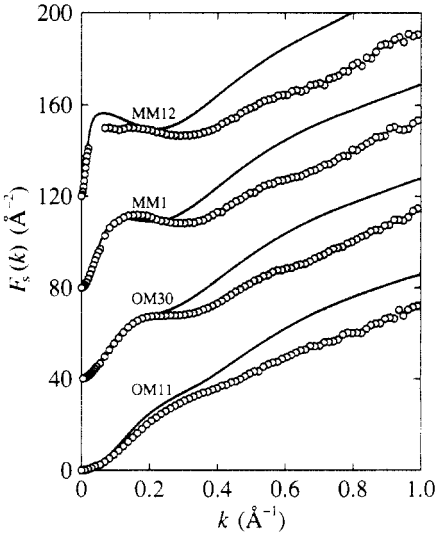

Figure 9. Comparison of the observed values of F_s with the HW theoretical values: (O) data in acetonitrile at 44.0 °C; (solid curves) best-fit HW theoretical values. The data points and theoretical curves for samples OM30, MM1, and MM12 are shifted upward by 40, 80, and 120 Å^{-2}, respectively.

for larger k and that the theoretical values of k at which F_s takes its maximum and minimum are always smaller than the observed values. Thus a theoretical curve such that in the range of large k its form is close to the experimental one is adopted as the "best-fit" theoretical curve, for convenience. In this case, the curve with λd = 0.06 is the best-fit one that may qualitatively reproduce the concave downward curvature observed at $k \simeq 0.55$ Å^{-1}.

As for the observed curvature (or inflection) mentioned above, it is pertinent to here refer to the previous theoretical results[14] presented in order to examine the effect of the discrete distribution of scattering centers, which has been evaluated on the basis of the HW Monte Carlo chain.[16] For the chain with the discrete scattering centers distributed along the contour corresponding to the α-carbon atoms, F_s has been shown to exhibit a small inflection at k = 0.35 Å^{-1}, which seems to correspond to the observed inflection (see Figure 1 of ref 14). As mentioned in the last subsection, the inflection that the RIS model predicts becomes weak as the number of rotational states is increased. Thus in the (continuous) limit of the infinitely large number of states, it may also predict the weak inflection as observed experimentally.

Now, Figure 9 shows plots of F_s against k for all the a-PMMA samples in acetonitrile at 44.0 °C. The unfilled

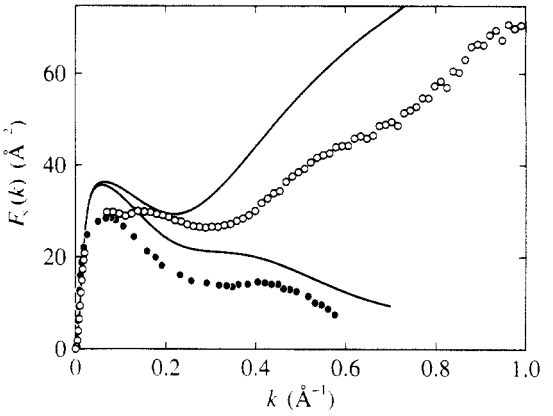

Figure 10. Effect of the distribution of scatterers: (O) present SAXS data for sample MM12 in acetonitrile at 44.0 °C; (●) SANS data by Dettenmaier et al.;[18] (solid curves) respective best-fit HW theoretical values with λd = 0.06 (upper) and λd = 0.24 (lower).

circles and solid curves represent the experimental data and the best-fit HW theoretical values calculated from eq 8 with eq 9 with the values of the model parameters mentioned above and with λd = 0.06, respectively. In the figure, the data points and theoretical curves for the samples OM30, MM1, and MM12 have been shifted upward by 40, 80, and 120 Å^{-2}, respectively. The theory may well reproduce the experimental data in the range of $k \lesssim 0.1$ Å^{-1} for the sample OM11, $k \lesssim 0.2$ Å^{-1} for OM30, $k \lesssim 0.1$ Å^{-1} for MM1, and $k \lesssim 0.05$ Å^{-1} for MM12. In the range of larger k, the theory explains qualitatively the behavior of the data, especially the concave downward curvature at $k \simeq 0.55$ Å^{-1}. In the present case for a-PMMA, the agreement between theory and experiment is only qualitative (or semiquantitative) as a whole, so that the precise determination of d as in the previous case of a-PS cannot be made. We only note that its value evaluated from the above values of λd and λ^{-1} is 2.8 Å, which is small, as expected.

It is interesting to here compare also the SANS data with the HW theory in order to examine the effect of the distribution of scatterers. The SANS data by Dettenmaier et al.[18] for the a-PMMA sample in Figure 7 have been reproduced in Figure 10 (filled circles), along with the present SAXS data for the sample MM12 (unfilled circles) and the corresponding HW theoretical values (upper solid curve with λd = 0.06) from Figure 9. The lower solid curve represents the HW theoretical values with λd = 0.24 corresponding to the SANS data. This value of λd has been chosen so that the theoretical curve may qualitatively explain the behavior of the SANS data, and we then obtain the value 11.3 Å of d. It is remarkably larger than the above value 2.8 Å evaluated from the SAXS data, as expected from the discussion in the last subsection. We note that the former value of d from SANS is rather close to the value 8.2 Å of the chain diameter evaluated from the partial specific volume[16] and also 7.2 Å of the hydrodynamic bead diameter evaluated from $[\eta]$.

Comparison with the a-PS Chain. Finally, we compare the present SAXS data for a-PMMA with the previous data for a-PS.[17] The data for the a-PMMA sample MM1 in acetonitrile at 44.0 °C (unfilled circles) along with the corresponding HW theoretical curve in Figure 9 have been reproduced in Figure 11. It includes the results reproduced from Figure 7 of ref 17 for an a-PS sample (F1-2) with $M_w = 1.01 \times 10^4$ in cyclohexane at 34.5 °C (Θ) (filled circles) along with the corresponding HW theoretical curve calculated with $\lambda^{-1}\kappa_0 = 3.0$, $\lambda^{-1}\tau_0 = 6.0$, $\lambda^{-1} = 22.5$ Å, $M_L = 36.7$ Å^{-1}, and $\lambda d = 0.61$.

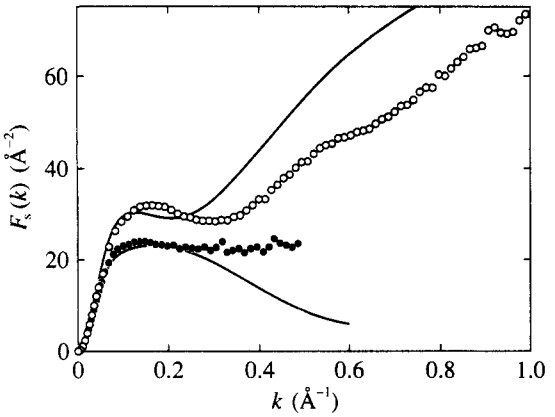

Figure 11. Comparison of the data for a-PMMA with those for a-PS: (○) present data for sample MM1 in acetonitrile at 44.0 °C; (●) previous data for an a-PS sample (F1-2) with $M_w = 1.01 \times 10^4$ in cyclohexane at 34.5 °C;[17] (solid curves) respective best-fit HW theoretical values.

The values of $\langle S^2\rangle_s^{1/2}$ determined in the previous studies[16,32] for the above a-PMMA and a-PS samples in their respective Θ solvents are 27.8 and 27.5 Å, respectively, and happen to be very close to each other. Reflecting this fact, the data for F_s for the two polymer samples are in excellent agreement with each other in the range of $k \lesssim 0.05$ Å^{-1}. We note that the values of $\langle S^2\rangle^{1/2}$ for these a-PMMA and a-PS samples are 27.6 and 27.3 Å,[16,32] respectively, and are very close to the respective values of $\langle S^2\rangle_s^{1/2}$, so that we need not distinguish $\langle S^2\rangle_s$ from $\langle S^2\rangle$ for $M_w \gtrsim 10^4$.

The observed and also calculated heights of the so-called plateau in the Kratky plot, which strictly cannot be observed for a-PMMA, are seen to be larger for a-PMMA than for a-PS. The behavior of F_s in this range of k (from ca. 0.05 to ca 0.2 Å^{-1}) may be considered to reflect the local chain conformation, since the effect of the electron distribution is rather small for $k \lesssim 0.2$. Thus it may be concluded that the HW theory may well explain in fact the observed difference in F_s between the two chains in such a range of k.

As for the plateau, however, we must note that a certain inconsistency occurs if the above SAXS data for the two polymers are analyzed on the basis of the Gaussian chain model. As is well known, F_s for this model is given by the Debye scattering function[33] and the height of its plateau is proportional to the ratio $M_w/\langle S^2\rangle$, thus leading to the conclusion that $\langle S^2\rangle$ is smaller for the a-PMMA chain than for the a-PS chain, the two chains having almost the same M_w. This is inconsistent with the above-mentioned fact that they have almost the same $\langle S^2\rangle$. Thus the Gaussian chain model is not valid for an analysis of SAXS data in this range, for which we must adopt a more realistic model, for instance, the HW chain model that may describe the local conformations.

The data for F_s in the range of $k \gtrsim 0.2$ Å^{-1} are strongly affected by the electron distribution. The difference between a-PMMA and a-PS in F_s there may be regarded as arising mainly from the fact that the thickness of the electron distribution around the chain contour is larger for a-PS than for a-PMMA. We note that for the letter, the effective thickness is so small that the shape of the Kratky plot is close to that for the chain with vanishing d.

Concluding Remarks

The scattering function P_s and therefore the Kratky function F_s for the unperturbed a-PMMA chains with various molecular weights, including the oligomers, each with the fraction of racemic diads $f_r = 0.79$, have been determined accurately in the range of $k < 1$ Å^{-1} by the use of a point-focusing SAXS camera in the High-Intensity X-ray Laboratory of Kyoto University. The Kratky plot of the data for the high-molecular-weight samples exhibits the first maximum and minimum as observed by Kirste and Wunderlich[1,2] for s-PMMA (with $f_r \simeq 0.9$) in benzene (good solvent). However, the former exhibits only a slight inflection in the range of large k, while the latter exhibits strong oscillation. Although on the basis of the RIS model[8,14,26] the behavior of F_s in the range of large k has been shown to depend in general on f_r, the difference between their and our data in such a range of k cannot be regarded as arising mainly from the difference in f_r between the PMMA samples used since their data for a-PMMA[2] also exhibit strong oscillation. A main source of the above disagreement may probably be due to the difference between their and our SAXS apparatuses and also that between the data processing procedures. For the confirmation of this conjecture, we plan to carry out SAXS measurements on s-PMMA samples with a point-focusing camera.

It has been shown that the HW theory may explain the experimental data quantitatively in the range of rather small k but only qualitatively in the range of large k. The reason for this disagreement between theory and experiment in the range of large k is not clear; at the present time, we have no idea for resolving this difficulty within the framework of the HW theory. However, it must be emphasized that the theory may give an explanation of the difference between the a-PMMA and a-PS chains in the behavior of F_s arising from that in the local conformation.

Acknowledgment. This research was supported in part by a Grant-in-Aid (01430018) from the Ministry of Education, Science, and Culture, Japan.

References and Notes

(1) Kirste, R. G.; Wunderlich, W. *Makromol. Chem.* **1964**, *73*, 240.
(2) Wunderlich, W.; Kirste, R. G. *Ber. Bunsen-Ges. Phys. Chem.* **1964**, *68*, 646.
(3) Kirste, R. G. *Makromol. Chem.* **1967**, *101*, 91.
(4) Kirste, R. G. In *Small-Angle X-Ray Scattering*; Brumberger, H., Ed.; Gordon and Breach: New York, 1967; p 33.
(5) Sundararajan, P. R.; Flory, P. J. *J. Am. Chem. Soc.* **1974**, *96*, 16.
(6) Yoon, D. Y.; Flory, P. J. *Polymer* **1975**, *16*, 645.
(7) Yoon, D. Y.; Flory, P. J. *Macromolecules* **1976**, *9*, 294.
(8) Yoon, D. Y.; Flory, P. J. *Macromolecules* **1976**, *9*, 299.
(9) Flory, P. J. *Statistical Mechanics of Chain Molecules*; Interscience: New York, 1969.
(10) Yamakawa, H. *Annu. Rev. Phys. Chem.* **1984**, *35*, 23.
(11) Yamakawa, H. In *Molecular Conformation and Dynamics of Macromolecules in Condensed Systems*; Nagasawa, M., Ed.; Elsevier: Amsterdam, 1988; p 21.
(12) Yamakawa, H.; Fujii, M. *J. Chem. Phys.* **1976**, *64*, 5222.
(13) Fujii, M.; Yamakawa, H. *J. Chem. Phys.* **1977**, *66*, 2578.
(14) Nagasaka, K.; Yoshizaki, T.; Shimada, J.; Yamakawa, H. *Macromolecules* **1991**, *24*, 924.
(15) Konishi, T.; Yoshizaki, T.; Shimada, J.; Yamakawa, H. *Macromolecules* **1989**, *22*, 1921 and succeeding papers.
(16) Tamai, Y.; Konishi, T.; Einaga, Y.; Fujii, M.; Yamakawa, H. *Macromolecules* **1990**, *23*, 4067.
(17) Koyama, H.; Yoshizaki, T.; Einaga, Y.; Hayashi, H.; Yamakawa, H. *Macromolecules* **1991**, *24*, 932.
(18) Dettenmaier, A.; Maconnachie, A.; Higgins, J. S.; Kausch, H. H.; Nguyen, T. Q. *Macromolecules* **1986**, *19*, 773.
(19) Fujii, Y.; Tamai, Y.; Konishi, T.; Yamakawa, H. *Macromolecules* **1991**, *24*, 1608.
(20) Hayashi, H.; Hamada, F.; Suehiro, S.; Masaki, N.; Ogawa, T.; Miyaji, H. *J. Appl. Crystallogr.* **1988**, *21*, 330.

(21) Yamakawa, H. *Modern Theory of Polymer Solutions*; Harper & Row: New York, 1971; p 211.
(22) Berry, G. C. *J. Chem. Phys.* **1966**, *44*, 4550.
(23) Kirste, R. G.; Kruse, W. A.; Ibel, K. *Polymer* **1975**, *16*, 120.
(24) Kirste, R. G.; Oberthür, R. C. In *Small-Angle X-Ray Scattering*; Glatter, O., Kratky, O., Eds.; Academic Press: New York, 1982; p 387.
(25) Sundararajan, P. R. *Macromolecules* **1986**, *19*, 415.
(26) Vacatello, M.; Yoon, D. Y.; Flory, P. J. *Macromolecules* **1990**, *23*, 1993.
(27) Vacatello, M.; Flory, P. J. *Macromolecules* **1986**, *19*, 405.
(28) O'Reilly, J. M.; Teegarden, D. M.; Wignall, G. D. *Macromolecules* **1985**, *18*, 2747.
(29) Ito, H.; Russell, T. P.; Wignall, G. D. *Macromolecules* **1987**, *20*, 2213.
(30) Yamakawa, H.; Shimada, J. *J. Chem. Phys.* **1979**, *70*, 609.
(31) Yamakawa, H.; Shimada, J.; Fujii, M. *J. Chem. Phys.* **1978**, *68*, 2140.
(32) Konishi, T.; Yoshizaki, T.; Saito, T.; Einaga, Y.; Yamakawa, H. *Macromolecules* **1990**, *23*, 290.
(33) Debye, P. *J. Phys. Colloid Chem.* **1947**, *51*, 18.